Phosphorus removal by steel slag filters: modeling dissolution and precipitation kinetics to predict longevity

*Dominique Claveau-Mallet**

Benoît Courcelles

Yves Comeau

Polytechnique Montreal, Department of Civil, Geological and Mining Engineering, Montreal (Quebec), Canada H3C 3A7

KEYWORDS

slag, phosphorus, wastewater treatment, PHREEQC, hydroxyapatite, model

ABSTRACT

This article presents an original numerical model suitable for longevity prediction of alkaline steel slag filters used for phosphorus removal. The model includes kinetic rates for slag dissolution, hydroxyapatite and monetite precipitation and for the transformation of monetite into hydroxyapatite. The model includes equations for slag exhaustion. Short-term batch tests using slag and continuous pH monitoring were conducted. The model parameters were calibrated on

these batch tests and experimental results were correctly reproduced. The model was then transposed to long-term continuous flow simulations using the software PHREEQC. Column simulations were run to test the effect of influent P concentration, influent inorganic C concentration and void hydraulic retention time on filter longevity and P retention capacity. High influent concentration of P and inorganic C, and low hydraulic retention time of voids reduced the filter longevity. The model provided realistic P breakthrough at the column outlet. Results were comparable to previous column experiments with the same slag regarding longevity and P retention capacity. A filter design methodology based on a simple batch test and numerical simulations is proposed.

INTRODUCTION

Slag filters are a promising technology for phosphorus (P) removal from wastewater. In the last 20 years, these passive systems were tested with success in different countries[1]. The large-scale utilization of slag filters, however, is inhibited by the limited number of full-scale implementations and the absence of mechanism based rather than empirical design methodology. Diverging results from various studies complicate the elaboration of a design strategy. The objective of this paper is to propose a model of phosphorus removal in alkaline steel slag filters. This model considers both longevity and efficiency of reactive filters.

The main mechanism for P removal observed in alkaline steel slag filters is the formation of hydroxyapatite (HAP), a stable calcium phosphate. HAP formation was observed in many previous studies[2-7]. Several metastable calcium phosphates such as brushite, monetite (MON) and octacalcium phosphate are precursors of HAP[8,9] and they were observed in slag filters[6,10]. HAP formation was the basis of a conceptual model presented by Claveau-Mallet et al.[2]. This conceptual model comprises three steps: (1) slag dissolution, (2) phosphorus precipitation and

crystal growth, and (3) P removal rate decrease caused by void filling particle accumulation and slag exhaustion. In the present project, this conceptual model is developed into a mathematical expression suitable for numerical simulations.

A challenge for the prediction of P removal is the disparity between batch test and continuous flow filter test results[11]. The proposed strategy is to characterize a given slag in a batch test and define parameters that are realistic in a filter test.

MATERIAL AND METHODS

The methodology involved two parts, batch test experiments with slag and numerical simulations.

Slag media. Electric arc furnace (EAF) slag from Arcelor Mittal located in Contrecoeur (QC) was used. The slag size was 5-10 mm and its density was 3.6 g/cm^3. The chemical composition of the slag was 33% Fe_2O_3, 30% CaO, 16% SiO_2 and 12% MgO. The same slag was used for phosphorus removal and mechanism studies in previous experiments[2,4,12-15].

Batch kinetic tests. A given amount of slag was placed in a 1L Erlenmeyer flask filled with 700 mL of solution (demineralised water or phosphorus solution). The Erlenmeyer was closed with a rubber cap connected with a nitrogen gas filled balloon to avoid exposure to atmosphere oxygen when sampling. A pH probe was inserted in the cap to allow continuous monitoring during tests. A syringe was used for water sampling by connecting it to a plastic tubing with a pinched valve inserted in the cap. Water samples were filtered at 0.45 microns and analyzed for ortho-phosphates (o-PO_4) and calcium. The temperature was controlled at 20°C and the Erlenmeyer was mixed on a gyratory shaker at 160 rpm, which produced movement of the slag at the bottom of the Erlenmeyer without suspension of the slag. The test lasted 3 to 7 days. The

effect of three parameters were tested in three experimental sets: initial phosphorus concentration, water/slag ratio and slag exhaustion.

o-PO_4 analyses were performed using a Lachat QuikChem 8500 flow injection analyzer using the ascorbic acid method[16]. Analyses of calcium were conducted with an AAnalyst 200 flame atomic absorption apparatus, using a standard mass spectrometry method[17].

Effect of initial phosphorus concentration. Initial phosphorus concentrations of 0, 10, 20 and 50 mg P/L were tested in the presence of a constant amount of slag of 35 g per flask. These concentrations were chosen as representative of concentrations met in real wastewaters. A fresh slag sample was used for each experiment. Phosphorus solutions were prepared using KH_2PO_4 and 30 mg/L of calcium added as $CaCl_2 \cdot 2H_2O$. Results obtained from these tests were used to calibrate the simulation model.

Effect of water/slag ratio. Slag masses of 35, 70, 350 and 700 g per flask were tested in distilled water. 700 g per flask was the highest amount of slag possible to add without affecting the probe. A fresh slag sample was used for each experiment. Test results were used to assess the effect of water/slag ratio on dissolution kinetics. The tested water/slag ratios were 1, 2, 10 and 20 mL/g. Reported water/slag ratio in various types of studies range from 0.33 mL/g in a slag filter with 50% porosity to 20 mL/g in leaching standard procedure tests[18].

Slag exhaustion. Tests were conducted at a constant initial phosphorus concentration of 45 mg P/L. A fresh slag sample of 350 g was used in a first batch test. The sample was then placed in a 0.08N HNO_3 "bath" solution for 24 h after which the solution pH was measured. The slag sample was then drained and used in a second test, which was followed by a second HNO_3 bath. The slag sample was submitted to 5 successive batch tests each followed by a HNO_3 bath. The

objective of this experimental set was to determine the effect of slag exhaustion (cumulative leached CaO, mol/g) on the rate of slag dissolution, a specific slag kinetic parameter.

PHREEQC modelling. PHREEQC is a free software commonly used for complex geochemical calculations[19]. PHREEQC includes equilibrium calculations, irreversible reactions, kinetic rates and mineral phases. The default PHREEQC Interactive 3.0 database was used. The main feature of the proposed model is to consider the kinetic rates of slag dissolution and of phosphorus precipitation in mineral phases. Slag dissolution was modeled as a simple CaO dissolution[2]. Two phosphorus mineral phases were included: HAP and MON. MON was chosen in the model to represent several amorphous or crystalline precursors in a single and simple expression. MON was preferred to other calcium phosphate species for its simple expression.

The transformation rate of metastable MON to the final stable phase HAP was included in the model.

Slag dissolution and phosphorus precipitation model and equations. The slag dissolution rate is defined by equation 1, where r_{diss} is the CaO dissolution rate (M/s), pH is the pH of water at any time and pH_{sat} is the saturation pH of the slag. k_{diss} (M/s) is the dissolution constant. pH_{sat} is defined as the maximum pH reached and k_{diss} is empirically determined by iterations (several simulations with various values of k_{diss} are run and the best fit is kept). The slag surface area is considered constant during the test.

$$r_{diss} = k_{diss}\left(\frac{pH_{sat}-pH}{pH_{sat}}\right) \quad (1)$$

The equation of HAP precipitation is given in equation 2. The rate of HAP precipitation (r_{HAP}, M/s) is expressed by a simple precipitation rate equation[20], where k_{HAP} (M/s) is a constant and SI_{HAP} is the saturation index of HAP in water (equation 3). This rate equation assumes a constant

temperature and specific surface area. SI_{HAP} is defined by equation 4, where K_{spHAP} is the solubility product of HAP.

$$5Ca^{2+} + 3PO_4^{3-} + OH^- \leftrightarrow Ca_5(PO_4)_3OH \quad (2)$$

$$r_{HAP} = k_{HAP}\, SI_{HAP} \quad (3)$$

$$SI_{HAP} = log\left(\frac{[Ca^{2+}]^5[PO_4^{3-}]^3[OH^-]}{K_{spHAP}}\right) \quad (4)$$

Equations of MON precipitation are similar to the ones for HAP (equations 5 to 7).

$$Ca^{2+} + HPO_4^{2-} \leftrightarrow CaHPO_4 \quad (5)$$

$$r_{MON} = k_{MON}\, SI_{MON} \quad (6)$$

$$SI_{MON} = log\left(\frac{[Ca^{2+}][HPO_4^{2-}]}{K_{spMON}}\right) \quad (7)$$

The transformation of MON to HAP is expressed in equation 8. The transformation rate ($r_{MONtoHAP}$, M/s) is a function of pH and of the remaining amount of MON (equation 9), and $k_{MONtoHAP}$ (M/s) is a constant determined by iterations. The transformation of MON to HAP was represented in PHREEQC by the addition of Ca^{2+} and OH^- to MON via the formation of $Ca(OH)_2$ (equation 10). Kinetic constants (k_{HAP}, k_{MON} and $k_{MONtoHAP}$) were determined empirically by iterations (several simulations with various values of k_{HAP}, k_{MON} and $k_{MONtoHAP}$ are run and the best fit is kept). Equilibrium constants (K_{spHAP}, 10^{-46} M^9 and K_{spMON}, 10^{-7} M^2) were chosen from the literature[8,21]. A discussion concerning the value of K_{spHAP} is provided in the result section.

$$3CaHPO_4 + 2Ca^{2+} + 4OH^- \rightarrow Ca_5(PO_4)_3OH + 3H_2O \quad (8)$$

$$r_{MON\ to\ HAP} = k_{MONtoHAP}\, pH\, MON \quad (9)$$

$$Ca^{2+} + 2OH^- \rightarrow Ca(OH)_2 \quad (10)$$

Precipitation phases included in the model are summarized in Table 1.

Table 1. Precipitation phases included in the model.

Phase	Formula	Log(k) (-)	Reference
HAP	$Ca_5(PO_4)_3OH$	-46	21
MON	$CaHPO_4$	-7	8

Batch simulations. The KINETICS data block of PHREEQC was used to simulate batch experiments. The four rates described in the last section were added in the RATES data block and dissolution parameters of slag (k_{diss} and pH_{sat}) were kept constant. Experimental initial solutions were represented using KH_2PO_4, $CaCl_2$ and CaO put in a pH 7 pure water with the REACTION data block, followed by an equilibrium at saturation index zero with HAP and MON in the EQUILIBRIUM_PHASES data block. No equilibrium with atmospheric CO_2 was done. Small amounts of CaO were added before the initial simulated solutions to reproduce initial experimental pH at time zero and the evolution of water properties (pH, calcium, phosphorus, amount of mineral phases) over time was computed by PHREEQC. From an experimental point of view, it was technically impossible to impose ideal initial conditions, which would mean that there is an instantaneous and homogenous contact between slag and water at time zero. Therefore, for simulations, a little amount of slag had already reacted before time zero of the test.

Simulation of column tests. The TRANSPORT data block was used to simulate water flow in a 1D column. The KINETICS and RATES data blocks were used for the definition of the four model rates. Inlet solutions were simulated in a similar way to batch tests: KH_2PO_4, K_2HPO_4, $CaCl_2$ and $NaHCO_3$ were added to a pH 7 pure water thought the REACTION data block, after which solutions were put into equilibrium with HAP and MON using the EQUILIBRIUM_PHASES data block. The column was divided into 10 cells that were 11 cm

thick each and a dispersivity of 1 cm (size of slag particles) was used[22]. A sensitivity analysis for dispersivity was performed with values of 0, 1, 2 and 5 cm (results presented as support information). The '-correct_disp' data block was set to true and flux boundary conditions were used at column's ends. Each cell had a total volume of 2 L with a porosity of 50%. The slag density was defined as 3.6 g/cm^3. The evolution of water properties over time within each column cell was computed by PHREEQC. The two dissolution parameters of slag k_{diss} and pH_{sat}, which were kept constant in batch simulations, were modified to account for the evolution of the slag/water ratio and of slag exhaustion. Constant values were replaced by exhaustion equations that were defined according to batch test results. Column simulations were run for 2000 void volumes, which were long enough to determine the column longevity. The column longevity was defined as the time at which the effluent phosphorus concentration increased to reach a value of 1 mg P/L. Other longevity definitions are possible (e. g. reach a given percentage of the influent concentration), but 1 mg P/L was chosen to represent a possible concentration requirement. The studied parameters (and tested values) were voids hydraulic retention time (HRT_V) (4, 8 and 16 h), influent phosphorus concentration (5, 6, 8, 10, 12, 14, 16, 18, 20, 22, 24, 26, 28 and 30 mg P/L) and influent $NaHCO_3$ concentration (0 and 0.5 mM). A total of 84 simulations were run.

RESULTS AND DISCUSSION

Batch test results: model application. Experimental and numerical results of batch tests are compared in Figure 1 for pH, P and Ca. Calibrated parameters were $k_{spHAP} = 10^{-46}\ M^9$, $k_{spMON} = 10^{-7}\ M^2$, $k_{MON} = 10^{-7}\ M/s$, $k_{HAP} = 10^{-8.6}\ M/s$, $k_{MONtoHAP} = 10^{-6}\ pH^{-1}s^{-1}$, $pH_{sat} = 11.52$ and $k_{diss} = 10^{-6.9\ \mp\ 0.4}\ M/s$. Experimental pH and phosphorus were accurately reproduced by the model and calcium was in the same range. Complex waves present in the pH experimental curves (e. g. 400 to 2000 min, curve 50 mg P/L, Figure 1A) resulting from the

cumulative effect of phosphoric acid buffers and phosphate calcium precipitations on hydroxide concentration were also accurately reproduced by the model.

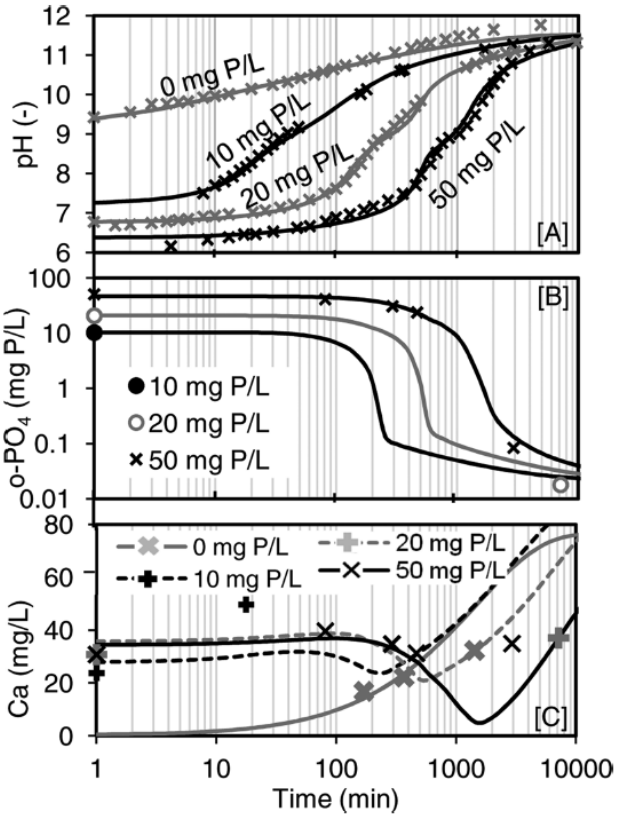

Figure 1: Comparison of batch test experimental and simulated results for pH (A), phosphorus (B) and calcium (C). Simulated results are epresented with lines and experimental results with circles, plus or X symbols.

The value of HAP solubility product used in the model ($k_{spHAP} = 10^{-46}\ M^9$) was higher then usual tabulated mineralogical data, which range from 10^{-55} to 10^{-63} M^9 [19,21,23]. The small size of freshly formed HAP crystals explains this difference. Surface energy influences solubility when the crystal size is smaller than 1 µm. The effect of specific surface on solubility product is given by the following equation[21]:

$$logK_{sp\_at\_S} = logK_{sp\_at\_S0} + \frac{\frac{2}{3}\bar{V}\,S}{2.3R\,T} \qquad (11)$$

where K_{sp} is the solubility product, S is the specific surface area (m^2/mol), $\bar{\gamma}$ is the mean free surface energy (87 mJ/m^2 for HAP), R is the ideal gas constant (8.31 J mol^{-1} K^{-1}) and T is the temperature (298 K). Using equation 11 and assuming a columnar crystal structure with a length/diameter ratio of 25/1, a crystal length of 0.016 μm and a bulk crystal solubility of 10^{-57} M[9], the solubility of finely grained HAP increased to 10^{-46} M[9]. Such values for crystal size and morphology were reported in previous studies[2,3]. Equation 11 explains why HAP supersaturation has been reported in alkaline slag filters[7].

For all simulated batch tests, the precipitation parameters of the model (k_{spHAP}, k_{spMON}, k_{MON}, k_{HAP} and $k_{MONtoHAP}$) had constant values (0, 10, 20 and 50 mg P/L initial phosphorus concentration) while the slag dissolution kinetic constant k_{diss} varied slightly between $10^{-6.4}$ and $10^{-7.2}$ M/s. This variation can be explained by the intrinsic composition variability of the slag. The expected presence of readily available CaO at the surface of slag particles increased the CaO dissolution rate of a given slag sample. This effect is important when 35 g slag samples are used in a batch test, as there are less than fifty slag particles in a sample. Therefore, it is important to test several slag sample replicates to assess the k_{diss} mean value and variability. The slag composition variability would probably be smaller if slag samples containing more particles were used. For subsequent column simulations, the mean value was used for $\log(k_{diss})$ to account for slag compositional variability.

Analysis of precipitation hypothesis. The model calibration presented in this study illustrates the importance of the precipitation hypothesis. Four simulations with different precipitation hypotheses were compared to experimental data (Figure 2A). The first hypothesis was based on a simple model which considers only the precipitation of HAP at equilibrium with $k_{spHAP} = 10^{-55.4} M^9$ (the value provided in the PHREEQC database). Simulation results did not reproduce

well the pH curve and the phosphorus concentration at the end of the simulation was too low (results not shown). The second model was similar to the first one, except for the value of k_{spHAP} which was increased to $10^{-46}M^9$. The resulting pH curve was closer to experimental data, but did not reproduce well the curve portion between 400 and 2000 minutes. The phosphorus simulated curve did not reproduce well the experimental data in the pH range of 7 to 9 (results not shown). In the third model, HAP precipitation kinetic was added, which improved the fit for both pH and phosphorus experimental curves. Finally, the fourth and complete model considering both HAP and MON formation fitted well for both pH and phosphorus (Figure 1). It was concluded that precipitation kinetics should be considered in a slag filter phosphorus removal model. A model based only on equilibrium phenomena is too simple and does not accurately represent reality.

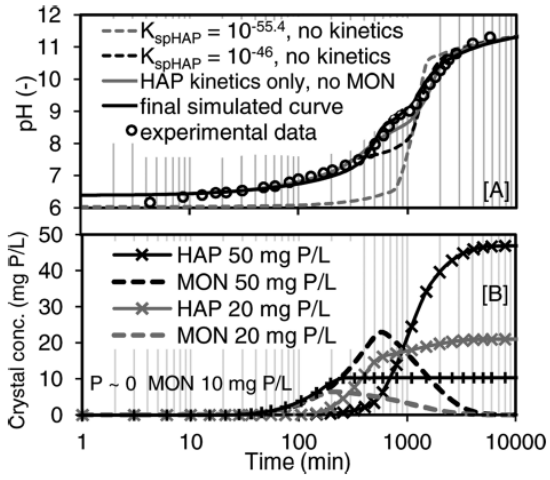

Figure 2: Effect of different precipitation hypotheses on simulated batch test results at an initial P concentration of 50 mg P/L (A) and evolution of phosphorus precipitates concentration in simulated batch tests (B).

Adding an intermediary precipitate as MON to the model improved its realism. Precipitation of HAP is significant only above pH 9, after which oversaturation rapidly increases. Thus,

precipitation of HAP alone does not explain the reduction of phosphorus in solution at intermediary pH (7 to 9), which was observed in the present and previous studies[2,3,7,24,25]. The addition of MON precipitation and transformation to HAP to the model was justified by previous studies. Several calcium phosphate precipitates are known to be metastable and to transform into HAP, which is stable[8]. This transformation phenomenon was qualitatively observed by scanning electronic microscopy and X-Ray diffraction in slag filter experiments[10] and bioceramic applications[9]. The evolution of HAP and MON concentration in simulations is shown in Figure 2B. MON had a lifetime of about 2000 minutes (33 hours), after which it was completely transformed into HAP. The simulated lifetime of MON is confirmed by Tsuru et al.[26], who observed an amorphous precipitate 1 to 3 days before the appearance of HAP in crystal growth experiments under neutral conditions. However, HAP started to precipitate faster in this study (after about 100 minutes). This was probably the result of alkaline conditions which favored HAP formation. Results of simulations indicated that transformation of MON into HAP is controlled by pH. Similar results were obtained in bioceramics applications under alkaline conditions with MON formation at neutral conditions. Le et al.[27] and Ito et al.[28] observed HAP at alkaline pH, and both HAP and MON at neutral conditions.

The ions used to define the HAP solubility product had major implications on simulation results. In our case, the solubility product of HAP was defined using the three ions Ca^{2+}, PO_4^{3-} and OH^-, as presented in equation 4. HAP solubility could have been defined differently using Ca^{2+}, HPO_4^{2-} and H^+ ions[19,23], or from Ca^{2+}, PO_4^{3-} and H^+ ions[7]. It would also be possible to add calcium-phosphate complexes such as $CaPO_4^-$ in the definition of the solubility product of HAP. In a model, only species stated in the solubility product contribute to the ionic product, and consequently, to the saturation index. In our model, calcium phosphorate complexes did not

contribute to the saturation index even if they were present in solution. Simulation results of this study showed that under steel slag filter conditions (high pH and high calcium concentration), soluble phosphorus is present mainly in the form of calcium complexes. Under relatively low pH conditions (e. g. pH of 8) and total calcium concentration of 27 mg/L, $CaPO_4^-$ and $CaHPO_4$ complexes represented 17% of soluble phosphorus. When the pH was higher (11.1) with the same calcium concentration (27 mg/L), $CaPO_4^-$ and $CaHPO_4$ complexes represented 98.3% of soluble phosphorus. When both pH and calcium were high (pH of 11.4 and calcium concentration of 250 mg/L), $CaPO_4^-$ and $CaHPO_4$ complexes represented 99.8% of soluble phosphorus. Therefore, the high pH and calcium concentration present in steel slag filters affects the fractionation of soluble phosphorus between calcium complexes and simple orthophosphates. This fractionation affects the modelled saturation index of HAP, as only PO_4^{3-} is considered as the soluble phosphate species. Further work is needed to assess the implication of soluble calcium phosphorus complexes in HAP precipitation to define a more realistic ion product that may include calcium phosphate complexes.

Using the model to predict filter longevity. *Batch test results: adaptation of model parameters to continuous flow filters.* The model that was used for batch test simulations could not be used directly for long term continuous flow column simulations as the behavior of slag dissolution differed between these two conditions. First, dissolution kinetics are faster in a column slag filter because its water to slag ratio is 0.3 mL/g (assuming a porosity of 50% and a slag grain density of 3.6), compared to 20 mL/g in batch tests. Second, slag is progressively exhausted in continuous flow slag column filters, a phenomenon that was not observed in batch tests. Consequently, the slag dissolution parameters of the model (k_{diss} and pH_{sat}) were modified to consider these two factors. The effect of water/slag ratio in batch tests is presented in Figure 3.

k_{diss} and pH_{sat} presented in this Figure were determined by calibration of their respective pH experimental curves with the proposed model. Relationships were used to extrapolate k_{diss} and pH_{sat} values from a ratio of 20 to a ratio of 0.3, which is the ratio present in slag filters. The resulting dissolution parameters for column simulations were $k_{diss} = 10^{-5.5} M/s$ and $pH_{sat} = 12.44$ which represent the initial dissolution behavior of slag without exhaustion.

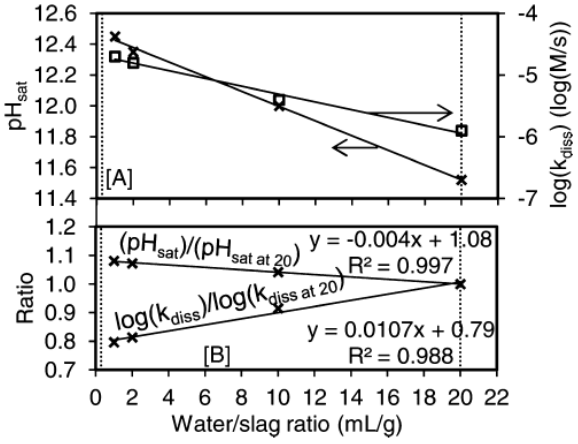

Figure 3: Effect of water/slag ratio on slag dissolution kinetic parameters. Dotted lines represent typical ratio values in slag filters (0.3 mL/g; left line) and standard batch tests (20 mL/g; right line).

Results of slag exhaustion batch tests are presented in Figure 4. These results illustrate the expected exhaustion of slag as pH_{sat} and k_{diss} progressively decrease. The proposed batch test is a simple methodology that indirectly considers various and complex slag properties including size, composition and initial presence of reactive powder on the slag surface. Initial dissolution parameters determined previously ($k_{diss} = 10^{-5.5} M/s$ and $pH_{sat} = 12.44$) were multiplied by relationships presented in Figure 4 to take into account the decrease in dissolution rate caused by slag exhaustion. The resulting dissolution parameters used in column tests are presented in equations 12 and 13. The A parameter was computed by PHREEQC at each time step within the

RATE modulus. The other precipitation parameters of the column slag filter model (k_{spHAP}, k_{spMON}, k_{MON}, k_{HAP} and $k_{MONtoHAP}$) remained identical to those of the batch test model.

$$\log(k_{diss}) = -5.5(365A + 1) \rightarrow k_{diss} = 10^{-1997A-5.5} \quad (12)$$

$$pH_{sat} = 12.44(4 \times 10^6 A^2 - 1670A + 1) \rightarrow pH_{sat} = 5.0 \times 10^7 A^2 - 20700A + 12.44 \quad (13)$$

where A is the cumulative amount of leached CaO (mol/g).

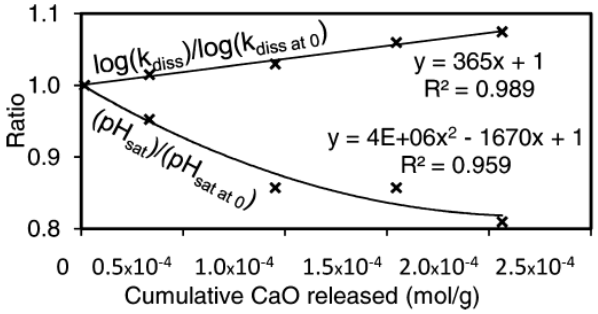

Figure 4: Slag dissolution exhaustion relationships.

Column modeling results. The simulated water composition at the column outlet is presented in Figure 5 for simulations with HRT_V = 16 h and influent $NaHCO_3$ concentration = 0. Results of all simulations are presented in a design graph in Figure 6.

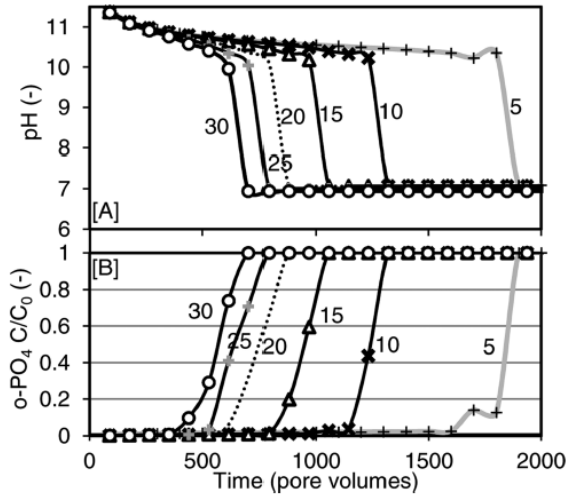

Figure 5: pH (A) and orthophosphates concentration (B) at the outlet of simulated column tests at HRTV = 16 h and influent NaHCO3 = 0, under various influent P concentrations. The influent P concentration (mg P/L) of each simulation is indicated next to its curve.

The same general trend was observed for all simulations. A good phosphorus removal efficiency at the beginning of operation was followed by a rapid decrease in efficiency. pH decreased slowly from 11 to 10, after which it rapidly dropped to 7 to 8, a trend that is typical of the behavior of real slag filters. A variation in inlet phosphorus concentration influenced the filter longevity, as shown in Figure 5. This result is explained by the buffer effect of phosphoric acid which exhausts slag. The addition of HCO_3 in the inlet water had a similar effect, reducing the filter longevity (Figure 6). The longevity reduction caused by influent HCO_3^- was more pronounced at low influent phosphorus concentration. A similar effect would be expected from the trapping of gaseous CO_2 if the liquid of the filter with its high pH were exposed to the atmosphere. A lower hydraulic retention time also reduced the filter longevity (Figure 6). A too short HRT_V resulted in an insufficient reaction time for slag dissolution and phosphorus precipitation. A high pH in the filter is a necessary but not a sufficient condition for phosphorus precipitation. Once the pH is raised above 10, time is needed for phosphorus precipitation as HAP to take place. This result provides an explanation for the wide orthophosphates concentration range (0.01 to 1 mg P/L) observed at high pH in slag filter effluents[3]. In practice, with the type of slag studied, maintaining a high pH is an essential indicator of an efficient P removal. o-PO_4 must be also monitored to ensure a low effluent value. In summary, for a given slag, the filter longevity depends on the composition of the inlet water (its buffer capacity) and on the HRT_V.

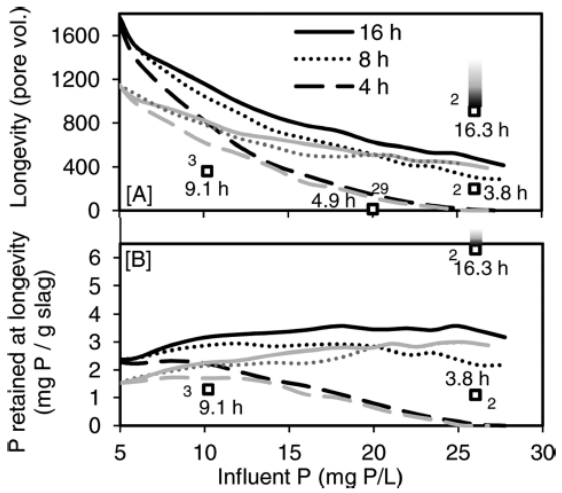

Figure 6: Design graph for prediction of longevity (A) and P retention at longevity (B) based on simulation results. Simulations with and without initial NaHCO3 are presented in gray and black, respectively. The HRTV is indicated in the legend. Experimental results from past studies are presented by squares or elongted squares to indicate that the longevity was greater than the value at the point. HRTV and reference are indicated next to each point.

Previous experimental works conducted in the authors' laboratory are compared to simulated results in Figure 6. Tests from these past studies were performed in saturated vertical columns fed from the bottom with synthetic wastewater (ref. 2 and 3) or with a real aquatic park effluent (ref. 29). The proposed design graph does reproduce these experimental results: it overestimates (ref. 3 and 29) or underestimates (ref. 2) them. Several reasons explain this difference. First, the slag used in ref. 3 was not the same batch as the one tested in the present study. The dissolution equations for that particular slag should be established following the proposed batch procedure to produce its own design graph. Second, the slag aging was not the same in ref. 2 and 29. Even if the slag was produced in the same steel mill using the same process, its reactivity can be greatly affected by weathering[14] and size[15]. Thus, kinetic parameters for a given slag with a given weathering should not be used for the same slag with a different weathering. Third, the

wastewater used in ref. 29 was a real wastewater containing salts, organic matter and inorganic carbon, which is not directly comparable with the design graph, that supposes a synthetic wastewater containing only inorganic phosphorus. Simulated results, nevertheless, remain in the same order of magnitude as those obtained experimentally for both longevity and retention capacity. Another factor that could explain the difference between simulations and experimental results is filter clogging, a factor discussed in a subsequent section.

This study proposes that the phosphorus removal performance of a slag filter is defined by two parameters: longevity and retention capacity at saturation. The proposed modelling strategy allows to calculate both values, which are important for design consideration. Longevity and retention capacity are not related by a simple and unique relationship. They are determined by the cumulative effect of the slag dissolution potential and precipitation kinetics, both of which are influenced by wastewater composition. As an example, a high influent phosphorus concentration increases the phosphorus retention capacity at saturation, but decreases longevity (Figure 5). A 70% reduction of HRT_V had a small influence on the retention capacity (decrease of only 7.5%) but a large effect on longevity (decrease of 26%). Finally, adding HCO_3 to the wastewater reduced the saturation capacity (Figure 5) because the pH-rise capacity of the slag was consumed by the carbonic acid.

Research needs. The proposed model needs to be improved and calibrated with experimental results before being used as a design tool. Its main shortcoming is the assumption that the contact between water and slag is never limited by the accumulation of particles, which is not realistic as clogging takes place due to particulate organic matter and various precipitates, notably HAP, other calcium phosphates and calcite. Particulate matter and precipitates prevent direct contact between slag surface and interstitial water, resulting in a reduced effective dissolution kinetic.

They also reduce filter porosity and the available time for reaction[30]. As an example, the initial porosity of 50% is reduced to 47% when longevity is reached for the base condition simulation (assuming an HAP density of 3.8 g/cm^3). Therefore, the proposed model effectively represents the maximum potential filter efficiency, a value that could not be reached in a real application. The proposed model needs to be completed to account for such clogging. A promising approach would be to couple a hydrodynamic code with a geochemical code, for example HYDRUS coupled with PHREEQC[31] or COMSOL coupled with PHREEQC[32]. The model also has to consider recovery properties that were observed in a previous study[12]. Recovery may be explained by our model as a reorganization of precipitates when the filter dries[2]. The more compact precipitate structure created increases contact between water and slag surface.

Specific recommendations are proposed to improve the model:

- Define more precisely the kinetic parameters. Batch tests could be run under different conditions (real wastewater, influent cations, known HAP growth inhibitors, etc.) to assess their specific effect on dissolution and precipitation kinetics[33]. The importance of MON in different stages of the filter operation could be assessed in batch tests containing HAP seeds. Statistical analyses should be conducted to evaluate the number of replicates that would be needed to correctly represent slag variability. The current proposed precipitation rates consider a constant specific surface which is unrealistic and additional work should be conducted to relate HAP growth rate to specific surface area[20].
- Add calcite precipitation within the slag filter model considering that calcite precipitation acts as a competitor to HAP precipitation[3,5]. Calcite formation can be a major concern in filters open to atmosphere.

- Consider the evolution of hydraulic conductivity and porosity for column simulations[30]. The evolution of these hydraulic properties is related to the total amount of precipitates and other particulate matters present in the filter. Precipitates should also be considered as a diffusion barrier for ions moving from the slag surface to interstitial water.
- The longitudinal and transverse dispersivity used in the model should be determined by tracer tests in experimental column tests. Several tracer tests should be conducted at different moments in the lifetime of the column to assess the effect of particle accumulation on dispersivity. Dispersivity could also be estimated from the media properties[34,35].
- Consider slag variability in a column simulation. In the present study, a constant k_{diss} was used. This constant value could be replaced by a distribution that would be determined by batch tests. The effect of different statistical distributions on simulation results should be assessed.
- Implement the model in a 2D or a 3D model. The model proposed in this paper is a 1D model that is valid only for plug flow systems such as long columns.

Practical design strategy for the prediction of slag filter longevity. The main contribution of this paper was to propose a prediction tool for slag filter longevity based on dissolution and precipitation kinetics. The proposed methodology is summarized in three steps:

1. Experimental batch tests. Each type of slag with specific composition and aging should be calibrated with the proposed batch tests prior to column simulations. First, slag should be sampled according to a standard procedure[36] to ensure representative sampling. Batch tests should be conducted in replicates with continuous pH monitoring and grab sampling for calcium and phosphorus analysis. Several tests should be

conducted with different ratios of slag to water. Exhaustion tests should be conducted. These tests should be conducted with distilled water and the real wastewater to be treated. The resulting kinetic parameters of the slag would be more reliable.

2. Numerical calibration of batch tests. Calibration of pH-rise curves should be conducted using the dissolution and precipitation model. Dissolution and precipitation kinetic constants can then be determined from which the exhaustion equation is defined. Grab P and calcium analyses should be used for the validation of the pH curve calibration.
3. Numerical simulations of filter. The longevity and retention capacity of the filter can then be predicted. Several HRT_V should be tested to optimize longevity and filter size.

Design strategies that can be applied to increase the longevity and retention capacity of the filter include using fresh (non weathered) slag, removing inorganic carbon upstream of the filter and increasing the HRT_V.

ASSOCIATED CONTENT

Supporting Information. A sensivity analysis for dispersivity was run with the following conditions: influent o-PO_4 = 27.7 mg P/L, influent $NaHCO_3$ = 0 and HRT_V = 8 h. This material is available free of charge via the Internet at http://pubs.acs.org.

AUTHOR INFORMATION

Corresponding Author

*dominique.claveau-mallet@polymtl.ca

ACKNOWLEDGMENTS

The authors warmly thank Denis Bouchard and Manon Leduc for chemical analyses and technical support, Claire Dacquin who worked on this project as an undergraduate intern, Denis

Marcotte for data analysis advices and Philippe Bouchard from Harsco for providing slag samples. This project was funded by the Natural Sciences and Engineering Research Council of Canada.

ABBREVIATIONS

HAP	Hydroxyapatite
HRT_V	Void hydraulic retention time (h)
k_{diss}	Slag dissolution kinetic constant (M CaO/s)
k_{HAP}	Hydroxyapatite precipitation kinetic constant (M HAP/s)
k_{MON}	Monetite precipitation kinetic constant (M MON/s)
$k_{MONtoHAP}$	Kinetic constant for the transformation of monetite to hydroxyapatite (M $Ca(OH)_2$(M MON s pH)$^{-1}$)
K_{spHAP}	Hydroxyapatite solubility product (M^9)
K_{spMON}	Monetite solubility product (M^2)
MON	Monetite
pH_{sat}	Slag saturation pH (-)
r_{diss}	Slag dissolution rate (M CaO/s)
r_{HAP}	Hydroxyapatite precipitation rate (M HAP/s)
r_{MON}	Monetite precipitation rate (M MON/s)
$r_{MONtoHAP}$	Monetite to hydroxyapatite transformation rate (M $Ca(OH)_2$/s)
SI_{HAP}	Saturation index of hydroxyapatite (-)
SI_{MON}	Saturation index of monetite (-)

REFERENCES

(1) Vohla, C.; Koiv, M.; Bavor, H. J.; Chazarenc, F.; Mander, U. Filter materials for phosphorus removal from wastewater in treatment wetlands - A review. *Ecol. Eng.* **2011**, 37 (1), 70-89.

(2) Claveau-Mallet, D.; Wallace, S.; Comeau, Y. Model of phosphorus precipitation and crystal formation in electric arc furnace steel slag filters. *Environ. Sci. Technol.* **2012**, 46 (3), 1465-1470.

(3) Claveau-Mallet, D.; Wallace, S.; Comeau, Y. Removal of phosphorus, fluoride and metals from a gypsum mining leachate using steel slag filters. *Water Res.* **2013,** 47 (4), 1512-1520.

(4) Drizo, A.; Forget, C.; Chapuis, R. P.; Comeau, Y. Phosphorus removal by electric arc furnace steel slag and serpentinite. *Water Res.* **2006,** 40 (8), 1547-1554.

(5) Liira, M.; Koiv, M.; Mander, U.; Motlep, R.; Vohla, C.; Kirsimae, K. Active filtration of phosphorus on Ca-rich hydrated oil shale ash: Does longer retention time improve the process? *Environ. Sci. Technol.* **2009,** 43 (10), 3809-3814.

(6) Kim, E.-H.; Yim, S.; Jung, H.-C.; Lee, E.-J. Hydroxyapatite crystallization from a highly concentrated phosphate solution using powdered converter slag as a seed material. *J. Haz. Mat.* **2006,** 136 (3), 690-697.

(7) Baker, M. J.; Blowes, D. W.; Ptacek, C. J. Laboratory development of permeable reactive mixtures for the removal of phosphorus from onsite wastewater disposal systems. *Environ. Sci. Technol.* **1998,** 32 (15), 2308-2316.

(8) Valsami-Jones, E. Mineralogical controls on phosphorus recovery from wastewaters. *Mineral. Mag.* **2001,** 65 (5), 611-620.

(9) Lundager Madsen, H. E. Influence of foreign metal ions on crystal growth and morphology of brushite ($CaHPO_4 \cdot 2H_2O$) and its transformation to octacalcium phosphate and apatite. *J. Cryst. Growth.* **2008,** 310 (10), 2602-2612.

(10) Bowden, L. I.; Jarvis, A. P.; Younger, P. L.; Johnson, K. L. Phosphorus removal from waste waters using basic oxygen steel slag. *Environ. Sci. Technol.* **2009,** 43 (7), 2476-2481.

(11) Chazarenc, F.; Kacem, M.; Gerente, C.; Andres, Y. 'Active' filters: a mini-review on the use of industrial by-products for upgrading phosphorus removal from treatment wetlands, In *Proc. 11th Int. Conf. on Wetland Systems for Water Pollution Control*, International Water Association, Nov. 1-7, Indore, India, **2008**.

(12) Drizo, A.; Comeau, Y.; Forget, C.; Chapuis, R. P. Phosphorus saturation potential: A parameter for estimating the longevity of constructed wetland systems. *Environ. Sci. Technol.* **2002,** 36 (21), 4642-4648.

(13) Mahadeo, K. Treatment of fish farm sludge supernatant with aerated filter beds and steel slag filters - Effect of organic matter and nutrient loading rates. Master Thesis, Polytechnique Montreal, 2013.

(14) Chazarenc, F.; Brisson, J.; Comeau, Y. Slag columns for upgrading phosphorus removal from constructed wetland effluents, In *Proc. Wetland Systems for Water Pollution Control X*, IWA Publishing, Sept. 23-29 2006, Lisbon, Portugal, **2007**.

(15) Abderraja Anjab, Z. Development of a steel slag bed for phosphorus removal from fishfarm wastewater. In french. Master Thesis (in french), Polytechnique Montreal, 2009.

(16) APHA, AWWA, WEF. *Standard methods for the examination of water and wastewater,* 22nd ed.; American Public Health Association, American Water Works Association, Water Environment Federation: Washington, D.C., 2012.

(17) Centre d'expertise en analyse environnementale du Québec. *Metals determination: method by mass spectrometry with argon plasma ionizing source.* In french. Centre d'expertise en analyse environmentale du Québec: MA. 200 - Mét 1.1, Ministère du développement durable, de l'environnement et des parcs du Québec, 2006.

(18) ASTM *Toxicity characteristic leaching procedure*; Am. Soc. Testing & Materials, West Conshohocken, PA, 1992.

(19) Parkhurst, David L.; Appelo, C. A. J. *User's guide to PHREEQC (Version 2) - A computer program for speciation, batch-reaction, one-dimensional transport, and inverse geochemical calculations*; U. S. Geological Survey: Denver, CO, 1999.

(20) Lasaga, A. C. Rate laws of chemical reactions. In *Kinetics of geochemical processes*; Mineralogical Society of America: Chelsea, MI, 1981.

(21) Stumm, W.; Morgan, J. J. *Aquatic Chemistry: Chemical Equilibria and Rates in Natural Waters;* 3rd ed.; John Wiley & Sons: New York, 1996.

(22) Domenico, P. A.; Schwartz, F. W. *Physical and Chemical Hydrogeology*; John Wiley & Sons: New York, 1998.

(23) Oelkers, E. H.; Bénézeth, P.; Pokrovski, G. S. Thermodynamic Databases for Water-Rock Interaction. In *Thermodynamics and kinetics of water-rock interaction.* Mineralogical Society of America and Geochemical Society: Chantilly, VA, 2009.

(24) Barca, C.; Troesch, S.; Meyer, D.; Drissen, P.; Andrès, Y.; Chazarenc, F. Steel Slag Filters to Upgrade Phosphorus Removal in Constructed Wetlands: Two Years of Field Experiments. *Environ. Sci. Technol.* **2013,** 47 (1), 549-556.

(25) Brient, S. Phosphorus removal from a fish farm wastewater with extensive steel slag fiters. In french. Master Thesis (in french), Polytechnique Montreal, 2012.

(26) Tsuru, K.; Kubo, M.; Hayakawa, S.; Ohtsuki, C.; Osaka, A. Kinetics of apatite deposition of silica gel dependent on the inorganic ion composition of simulated body fluids. *J. Ceram. Soc. Jap.* **2001,** 109 (1269), 412-418.

(27) Le, H. R.; Chen, K. Y.; Wang, C. A. Effect of pH and temperature on the morphology and phases of co-precipitated hydroxyapatite. *J. Sol-Gel Sci. Technol.* **2012,** 61 (3), 592-599.

(28) Ito, H.; Oaki, Y.; Imai, H. Selective Synthesis of Various Nanoscale Morphologies of Hydroxyapatite via an Intermediate phase. *Cryst. Growth & Des.* **2008,** 8 (3), 1055-1059.

(29) Vallet, B. Phosphorus removal of the Montreal Biodome Saint-Laurent Marin basin by steel slag. Intern Report (in french), Polytechnique Montreal, 2001.

(30) Courcelles, B.; Modaressi-Farahmand-Razavi, A.; Gouvenot, D.; Esnault-Filet, A. Influence of precipitates on hydraulic performance of permeable reactive barrier filters. *Intern. J. Geomech.* **2011,** 11 (2), 142-151.

(31) PC-Progress Website; Hydrus-1D for Windows, Version 4.xx, consulted on May 9th 2014, hydrus. http://www.pc-progress.com/en/Default.aspx?hydrus-1d

(32) Comsol Website; consulted on May 9th 2014, http://www.comsol.com/

(33) Cucarella, V.; Renman, G. Phosphorus sorption capacity of filter materials used for on-site wastewater treatment determined in batch experiments - a comparative study. *J. Environ. Qual.* **2009**, 38(2), 381-392.

(34) Delgado, J. M. P. Q. A critical review of dispersion in packed beds. *Heat Mass Transf.* **2006**, 42(4), 279-310.

(35) Jourak, A.; Frishfelds, V.; Hellström, J. G.; Lundström, T. S.; Herrmann, I.; Hedström, A. Longitudinal dispersion coefficient: effects of particle-size distribution. *Transp. Por. Med.* **2013**, 99(1), 1-16.

(36) *ASTM C 702 / C 702 M−11 Standard Practice for Reducing Samples of Aggregate to Testing Size*; Am. Soc. Testing & Materials, West Conshohocken, PA, 2011.